



Novel organotin-PTA complexes supported on mesoporous carbon materials as recyclable catalysts for solvent-free cyanosilylation of aldehydes

Abdallah G. Mahmoud^{a,b,*}, Ivy L. Librando^{a,c}, Anup Paul^{a,**}, Sónia A.C. Carabineiro^{a,d,e,*}, Ana Maria Ferraria^{f,g,h}, Ana Maria Botelho do Rego^{f,g,h}, M.Fátima C. Guedes da Silva^{a,h}, Carlos F.G.C. Geraldes^{i,j}, Armando J.L. Pombeiro^{a,k}

^a Centro de Química Estrutural, Institute of Molecular Sciences, Instituto Superior Técnico, Universidade de Lisboa, Av. Rovisco Pais, 1049-001 Lisboa, Portugal

^b Department of Chemistry, Faculty of Science, Helwan University, Ain Helwan, Cairo 11795, Egypt

^c Department of Chemistry, Mindanao State University-Iligan Institute of Technology, Tibanga, Iligan City 9200, Philippines

^d LAQV-REQUIMTE, Department of Chemistry, Nova School of Science and Technology, Universidade Nova de Lisboa, 2829-516 Caparica, Portugal

^e LSRE-LCM – Laboratory of Separation and Reaction Engineering – Laboratory of Catalysis and Materials, Faculty of Engineering, University of Porto, Rua Dr. Roberto Frias, 4200-465 Porto, Portugal

^f BSIRG, IBB - Institute for Bioengineering and Biosciences, Instituto Superior Técnico, Universidade de Lisboa, 1049-001 Lisboa, Portugal

^g Associate Laboratory i4HB—Institute for Health and Bioeconomy at Instituto Superior Técnico, Universidade de Lisboa, Av. Rovisco Pais, 1049-001 Lisboa, Portugal

^h Departamento de Engenharia Química, Instituto Superior Técnico, Universidade de Lisboa, Av. Rovisco Pais, 1049-001 Lisboa, Portugal

ⁱ Department of Life Sciences, Faculty of Science and Technology, Calçada Martim de Freitas, 3000-393 Coimbra, Portugal

^j Coimbra Chemistry Center, University of Coimbra, Rua Larga Largo D. Dinis, 3004-535 Coimbra, Portugal

^k Peoples' Friendship University of Russia (RUDN University), Research Institute of Chemistry, 6 Miklukho-Maklaya Street, Moscow 117198, Russian Federation

ARTICLE INFO

Keywords:

Cyanosilylation
Carbon materials
Heterogeneous catalysis
1,3,5-triaza-7-phosphaadamantane
Microwave
Tetrel σ -hole bond

ABSTRACT

New organotin compounds with general formula $[(\text{PTA-CH}_2\text{-C}_6\text{H}_4\text{-p-COO})\text{SnR}_3]\text{Br}$ (where R is Me for **3** and Ph for **4**; PTA = 1,3,5-triaza-7-phosphaadamantane), bearing the methylene benzoate PTA derivative, were synthesized through a mild two-step process. The compounds were characterized by Fourier transform infrared spectroscopy, electrospray ionization mass spectrometry, elemental analysis and nuclear magnetic resonance spectroscopy (NMR). They were heterogenized on commercially available activated carbon (AC) and multi-walled carbon nanotubes (CNT), as well as on their chemically modified analogues. The obtained materials were characterized by scanning electron microscopy, transmission electron microscopy and X-ray photoelectron spectroscopy. Complex **3** supported on activated carbon (**3-AC**) was found to be an active and recyclable catalyst for the cyanosilylation of several aromatic and aliphatic aldehydes. Using **3-AC** with a low loading of 0.1 mol% several substrates were quantitatively converted, within just 5 min at 50 °C and under microwave irradiation in solvent-free conditions. Multinuclear NMR analysis suggested a mechanism that potentially involves a double activation process, where the nucleophilic phosphorus at the PTA derivative acts as a Lewis base and the Sn(IV) metal centre as a Lewis acid.

1. Introduction

Cyanohydrins are versatile intermediates in synthetic chemistry that can be conveniently converted into a wide range of building blocks, such

as α -hydroxy acids, α -hydroxy ketones, α -amino acids and β -amino alcohols, for the agricultural and pharmaceutical industries [1–5]. One of the most fundamental and efficient methods for obtaining cyanohydrins is through the catalytic cyanosilylation of aldehydes using trimethylsilyl

* Corresponding authors at: Centro de Química Estrutural, Institute of Molecular Sciences, Instituto Superior Técnico, Universidade de Lisboa, Av. Rovisco Pais, 1049-001 Lisboa, Portugal.

** Corresponding author.

E-mail addresses: Abdallah.mahmoud@tecnico.ulisboa.pt (A.G. Mahmoud), anuppaul@tecnico.ulisboa.pt (A. Paul), sonia.carabineiro@fct.unl.pt (S.A.C. Carabineiro).

<https://doi.org/10.1016/j.cattod.2023.114270>

Received 17 February 2023; Received in revised form 24 May 2023; Accepted 13 June 2023

Available online 16 June 2023

0920-5861/© 2023 The Authors. Published by Elsevier B.V. This is an open access article under the CC BY-NC-ND license (<http://creativecommons.org/licenses/by-nc-nd/4.0/>).

cyanide (TMSCN) as the cyanide source (Scheme 1) [4,5].

Transition and main-group metal complexes with Lewis acid character have been intensively used as homogenous catalysts for cyanosilylation reactions [6–9]. The difficulty of separation and recycling of such catalysts remains the main obstacle for their utilization on an industrial large-scale. To overcome this limitation, the use of recyclable carbon-anchored metal complexes as heterogeneous catalysts is a more practical and economical alternative. However, reported examples of this approach are scarce [10,11].

The coordination chemistry of organotin compounds has garnered much attention due to their industrial applications as heat/light stabilizers [12–14] and catalysts [15–19] for various organic transformations. Despite the significant advantages in terms of catalyst recovery and recycling, there are only a few studies of highly active heterogeneous catalysts based on organotin complexes for aldehyde cyanosilylation reaction [20,21].

The cage-like monophosphine 1,3,5-triaza-7-phosphadamantane (PTA) and its derivatives have gained a renewed and growing interest in the field of organometallic chemistry for their air-stability and neutral donor properties, with a wide range of applications including catalysis, medicinal inorganic chemistry and as photoluminescent materials [22–26]. However, the soft base nature of the P coordination site limits its complexes to soft transition metals, and complexes involving hard post-transition metals with PTA moieties are yet to be reported [23,24].

Pursuing our interest on studying metal-PTA complexes [27–32] and their carbon-supported catalysts for organic transformations [31–33], herein, we report, for the first time, the synthesis and characterization of two novel Sn(IV) organometallic compounds bearing a *N*-methylenebenzoate PTA derivative, PTA-CH₂-C₆H₄-*p*-COO⁻. The compounds were heterogenized on activated carbon (AC) and multi-walled carbon nanotubes (CNT) to be used as active, rapid and recyclable catalysts for microwave assisted cyanosilylation of aldehydes in solvent-free conditions.

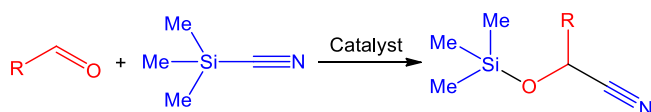
2. Results and discussion

2.1. Synthesis and characterization of the complexes

The preparation of organotin compounds with the *N*-functionalized PTA ligand involves a two-step process (Scheme 2). The first step was carried out by mixing 4-(bromomethyl)benzoic acid and R₃SnOH (R = methyl or phenyl) in toluene under reflux to produce the bromomethylenebenzoate tin(IV) complexes **1** and **2**, respectively. The second step involves reacting an equimolar amount of PTA with **1** or **2** in acetone, which results in the formation of the *N*-alkylated PTA cationic complexes with the general formula [(PTA-CH₂-C₆H₄-*p*-COO)SnR₃]Br (R = Me for **3** and Ph for **4**). The air-stable compounds **3** and **4** are hydrosoluble due to their ammonium salt functionality. The proposed formulations of the obtained compounds **1–4** were confirmed using Fourier-transform infrared spectroscopy (FTIR), elemental analysis, nuclear magnetic resonance (NMR) spectroscopy (¹H, ¹³C{¹H}, ³¹P{¹H} and ¹¹⁹Sn{¹H}); Figs. S1–S18) and electrospray ionization mass spectrometry (ESI-MS).

The distinctive bands of the asymmetric ν_{asym}(OCO) and symmetric ν_{sym}(OCO) stretching vibrations of the carboxylate group are shown in the FTIR spectra of triorganotin(IV) compounds **1** and **2** at 1600–1617 and 1350–1430 cm⁻¹, respectively, demonstrating the anisobidentate coordination with organotin fragments (Figs. S19 and S20). [34–36].

The *N*-alkylation of PTA results in a complex pattern for the



Scheme 1. Cyanosilylation reaction of aldehyde.

methylene protons in the ¹H NMR spectra of compounds **3** and **4**. Additionally, these spectra show the presence of the aromatic moieties in the 8.00–7.30 ppm range. The protons of the trimethyl tin group in **3** are observed at δ 0.5.

The four signals in the aromatic region of the ¹³C{¹H} NMR spectra of compounds **3** and **4** confirm the presence of the methylenebenzoate moieties. More aromatic resonances are observed in the spectrum of compound **4** due to the presence of the -Sn(Ph)₃ phenyl rings. The presence of four methylene carbon signals was also detected; those corresponding to N-CH₂-N and N-CH₂-N⁺ emerge as singlets, while those of P-CH₂-N and P-CH₂-N⁺ appear as doublets due to first order J_{P-C} coupling.

The ³¹P{¹H} NMR spectra show a sharp singlet at δ – 83.55 for **3** and at δ – 83.67 for **4**. The ¹¹⁹Sn{¹H} NMR spectra confirm the presence of a single tin species in **3** and **4**, through singlets at δ – 19.65 and δ – 326.43, respectively.

The ¹¹⁹Sn{¹H} NMR spectra of compounds **1** and **3** exhibit a singlet at – 15.31 and – 19.65 ppm, respectively, suggesting a tetracoordinated Sn(IV) environment (Figs. S2 and S7). [37] While compounds **2** and **4** exhibit a singlet at – 230.52 and – 326.43 ppm, respectively, suggesting a pentacoordinated Sn(IV) environment (Figs. S4 and S14). [38–40].

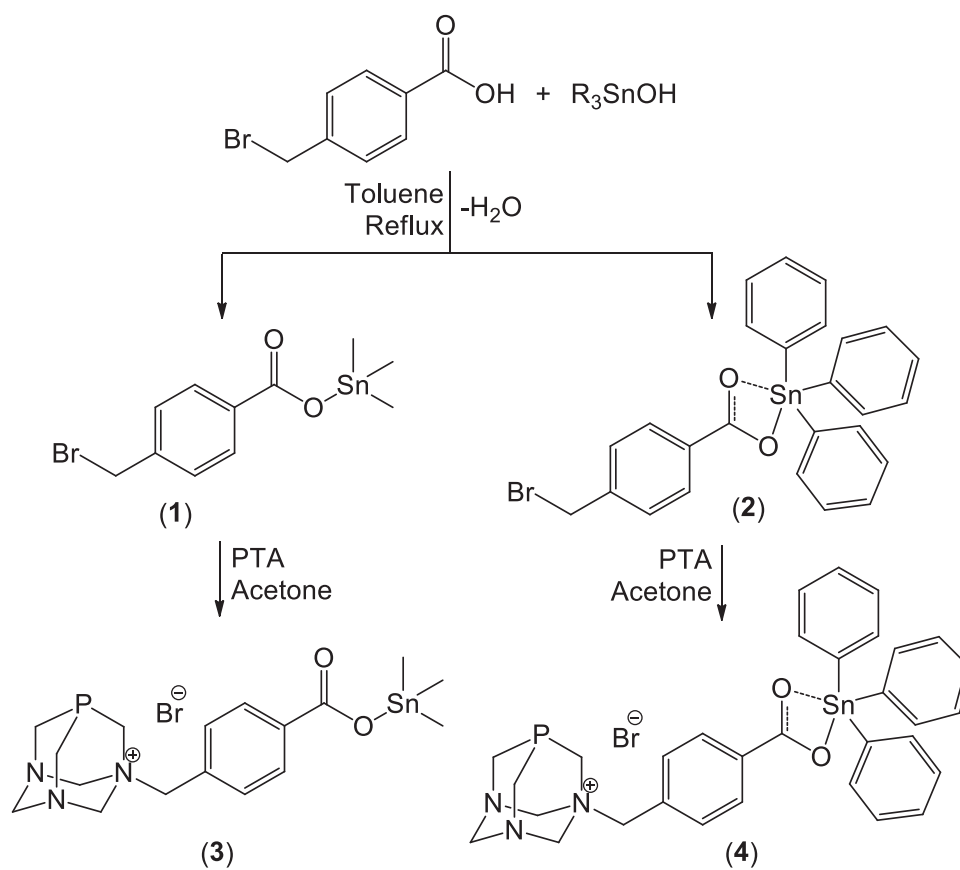
2.2. Preparation and characterization of the heterogenized catalysts

Activated carbon (AC, from Sigma–Aldrich Norit RO 0.8) and multi-walled carbon nanotubes (CNT, Nanocyl NC3100) were used as solid supports, as in a previous work [41]. The oxidized AC-ox and CNT-ox materials were obtained from their pristine analogues by reaction with nitric acid (5 M) under reflux. These were then treated with sodium hydroxide (20 mM) to achieve the AC-ox-Na and CNT-ox-Na carbon supports.

The morphologies of the carbon supports used in this work were analysed by scanning electron microscopy (SEM) and transmission electron microscopy (TEM). The SEM images of AC-based materials show distinct pores, as shown in Fig. 1a–c. The general morphology of the AC materials does not differ significantly, but AC-ox-Na (Fig. 1c) contains several smaller pores compared to commercial AC and AC-ox materials. The morphologies of the modified CNT materials (Fig. 1e–f) are not much different from that of pristine CNT (Fig. 1d). The aggregated threadlike appearance of CNTs creates pores as a result of the 3D stacking of the fibres. The SEM images of **3**-AC (Fig. 2) show a thick, fragmented plate-like structure covered with small off-white debris. This appearance may be due to the complex being immobilized on the surfaces of the support material. The TEM micrographs of complex **3** on carbon materials are shown in Fig. 3a–f. Darkened areas can be seen in the supports which could indicate the presence of severe particle aggregation in the catalysts. Furthermore, the morphology of AC-based catalysts displays stacked disc-shaped crystallites, while CNT-based unveils threadlike structures.

The surface properties of the carbon supports were investigated by N₂ adsorption measurements at – 196 °C, after degassing the samples at 150 °C under dynamic vacuum. The results are presented in Table 1. The BET surface areas of the carbon supports were found to be in the range of 361–866 m²/g, with the AC materials having higher surface areas.

The mesoporous character of the carbon materials was confirmed with the shapes of their nitrogen adsorption-desorption isotherms depicted in Figs. S21 and S22. According to the IUPAC classification of isotherms, the AC and its chemically modified analogues exhibit type II isotherm (Fig. S21), characteristic of monolayer-multilayer adsorption on an open and stable powder external surface. Their full adsorption-desorption isotherms show type H3 hysteresis, which are obtained with aggregates of plate-like particles (as concluded from the SEM images depicted in Figs. 1a–c and 2) that possess non-rigid slit-shaped pores. On the other hand, CNTs show type IV isotherms (Fig. S22) confined to the adsorption process via multilayer adsorption followed



Scheme 2. Synthesis of complexes 1-4.

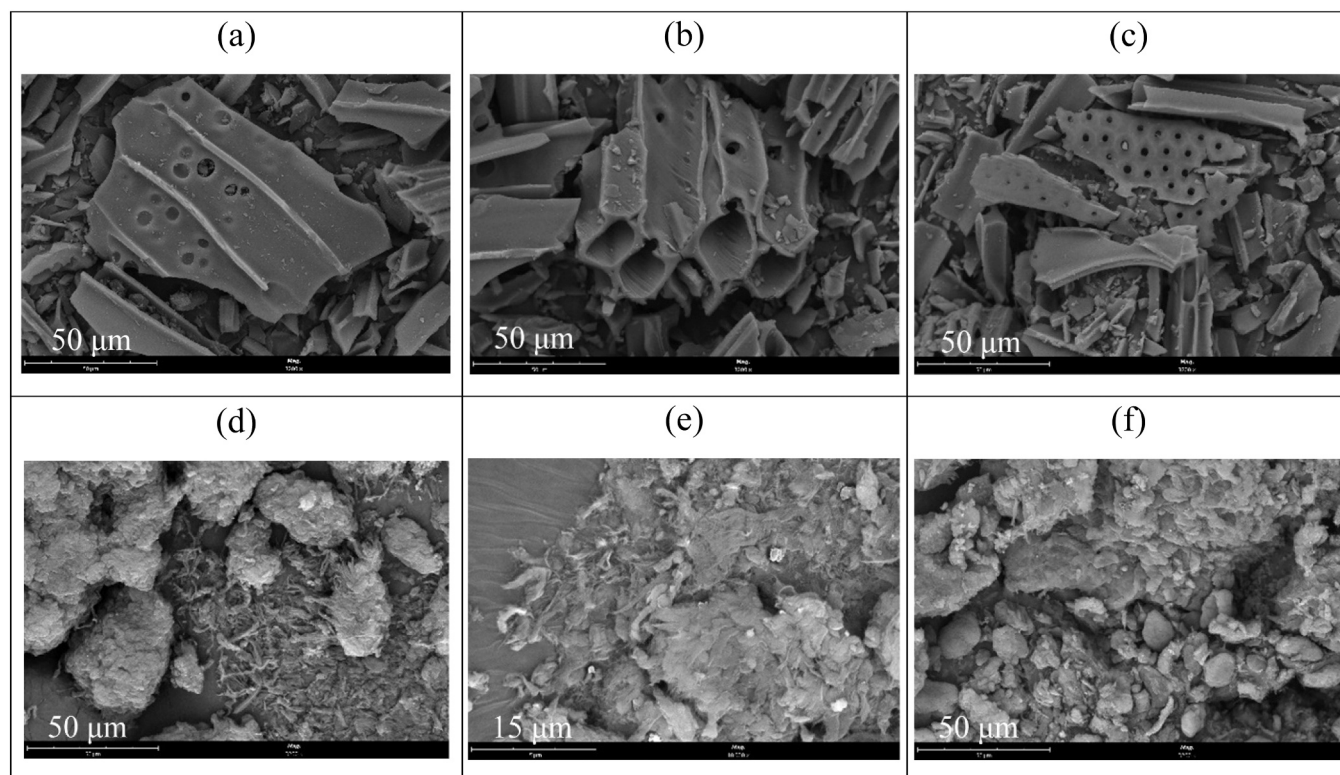


Fig. 1. SEM images of carbon supports: (a) AC, (b) AC-ox, (c) AC-ox-Na, (d) CNT, (e) CNT-ox, and (f) CNT-ox-Na.

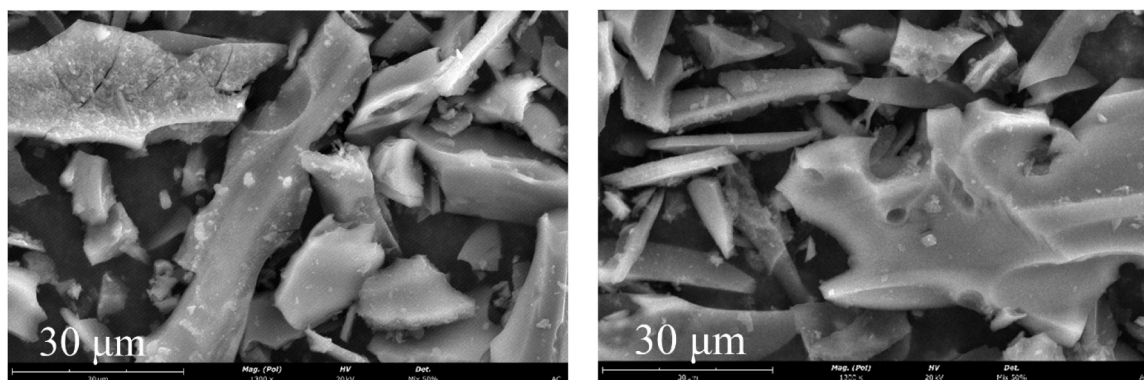


Fig. 2. SEM micrographs of 3-AC.

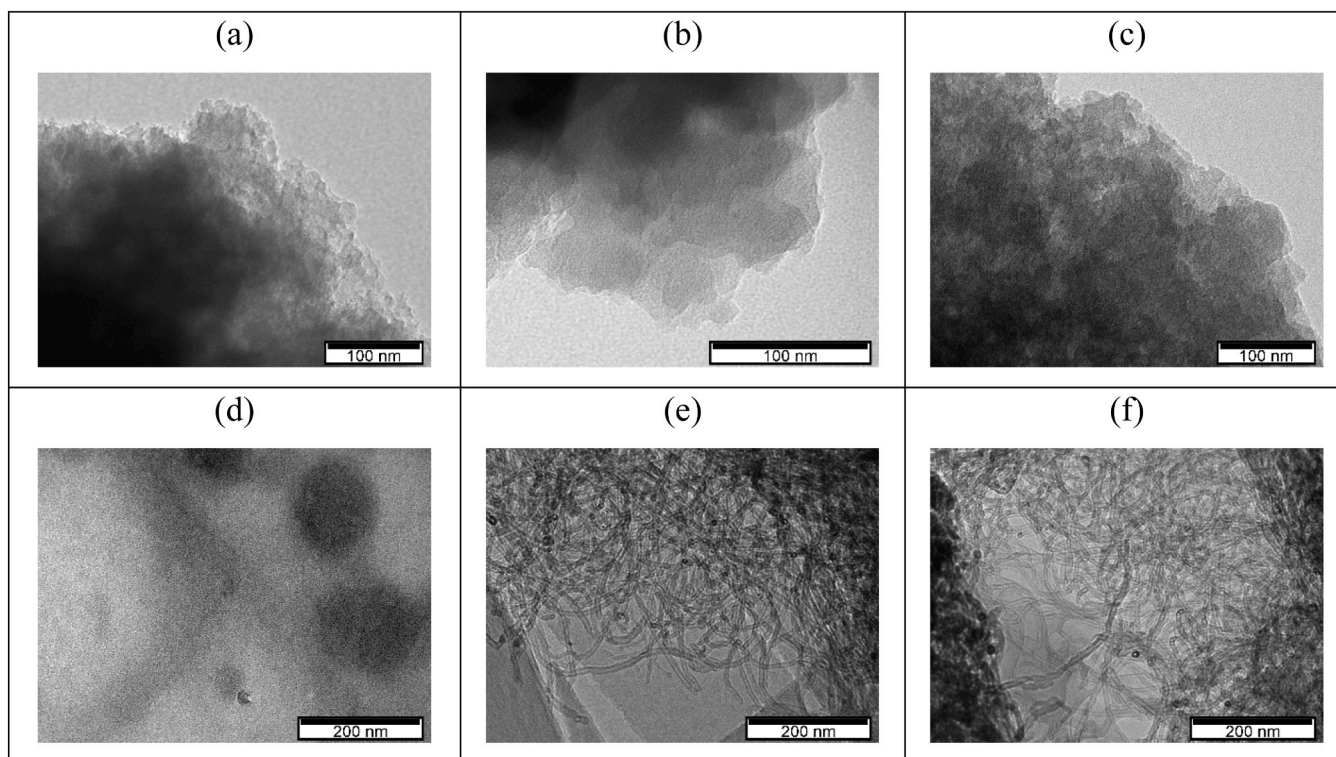


Fig. 3. The TEM morphology of complex 3 immobilized on (a) AC (b) AC-ox (c) AC-ox-Na (d) CNT (e) CNT-ox (f) CNT-ox-Na.

Table 1

Characterization of carbon materials by adsorption of N_2 at -196 °C: surface area (S_{BET}), total pore volume (V_p), micropore volume (V_{mic}), average pore size (d). Amounts of CO and CO_2 desorbed (previously determined by temperature programmed desorption (TPD) [41]).

Carbon support	S_{BET} $m^2 g^{-1}$	V_p $cm^3 g^{-1}$	V_{mic} $cm^3 g^{-1}$	d nm	CO $\mu mol g^{-1}$	CO_2 $\mu mol g^{-1}$
AC	866	0.45	0.22	5.2	643	179
AC-ox	724	0.31	0.19	4.6	4930	2596
AC-ox-Na	477	0.18	0.13	4.7	5012	2883
CNT	302	2.85	0.01	30.3	142	89
CNT-ox	301	1.62	0.006	19.0	1475	729
CNT-ox-Na	261	1.21	0.005	16.5	1079	838

with capillary condensation. The observed hysteresis loop is close to H1 type, which is associated with the cylindrical pore geometry and high degree of pore size uniformity.[42].

The amounts of released CO and CO_2 gases were determined using

temperature-programmed desorption (TPD) method and the corresponding curves are also shown in Fig. S23. The TPD results showed that the pristine carbon supports had low levels of CO and CO_2 released, indicating a high degree of graphitization and stability of the materials. The AC supports were found to be microporous with a rich surface chemistry, having more surface groups than CNT. Upon functionalization, larger amounts of CO and CO_2 were released from the AC and CNT materials, indicating the decomposition of surface groups formed during the activation process, such as carboxylic acids, anhydrides, lactones, phenol and carbonyls formed during the activation process.[41,43,44] The nitric acid oxidation treatment increased the carboxylic acid groups on the -ox materials, which were then transformed into phenolates and carboxylates upon NaOH treatment to obtain the -ox-Na materials [41, 43,44]. Overall, the analysis of the carbon supports confirms their appropriateness for the immobilization of the tin complexes.

The immobilization of complexes 3 and 4 on the carbon supports was performed by dissolving the compounds in water, followed by the addition of the carbon materials and stirring the mixture for 72 h at

room temperature. The amounts of the compounds heterogenized on the carbon supports were determined by measuring the tin metal loading through inductively coupled plasma-atomic emission spectroscopy (ICP-AES) analysis (Table 2). The results show that both complexes were successfully anchored on the surface of the carbon supports, with compound **3** being immobilized more efficiently, which could be attributed to the bulkiness of compound **4** bearing three phenyl rings. Among the carbon supports, the AC materials have higher loading values compared to the CNTs. The surface-modified analogues have better heterogenization efficiency than the pristine materials, which implies that the complexes anchor more effectively on surfaces with an increased number of functional groups brought by surface treatments.

The carbon materials loaded with Sn complex **3** were also characterised by nitrogen adsorption-desorption measurements (Table S1) to compare their surface features with those of the initial carbon materials (Table 1). In general, the surface parameters of the carbon materials loaded with **3**, such as BET surface area, pore size and pore volume, exhibit much lower values when compared to their free analogues. This indicates that the complex is efficiently anchored not only on the outer surface of the supports but also inside the pores.

The immobilization of **3** on AC was studied by XPS. Fig. 4 shows the XPS spectra of AC, **3** and **3-AC**. The carbon support, AC, and **3** were also analysed for comparison purposes. The AC shows the typical spectrum of a graphitized carbon with the C 1s region fitted with an intense peak centred at 284.7 eV assigned to sp² carbon atoms and an energy loss region, from π-π* electron excitations associated to a delocalized system, that extends roughly from 288 eV to 293 eV (Fig. 4a). Some oxidised carbon functionalities (C-O, C=O or COOH) are overlapping the vibronic fine structure, responsible for the asymmetric profile of C 1s [45], and the π-π* excitation features. A residual relative amount of nitrogen is also detected (Table 3): N 1s was fitted with a single peak centred at 401.4 eV attributed to protonated amines (Fig. 4c and Table S2). The C 1s region of **3** was fitted with five peaks centred at binding energies (BE) compatible with the chemical structure of **3** predicted in Scheme 2. However, an additional peak assigned to carbon bonded to oxygen was needed to obtain a reliable fitting. Actually, this sample shows an excess of oxygen (cf. O/C in Table 3) compatible with the presence of retained acetone. Surprisingly, in **3**, P 2p region that should include only one doublet assigned to the phosphorus atom, has the contribution of two doublets with spin-orbit separations of 0.87 eV and P 2p_{3/2} components centred at 130.8 eV and 132.6 eV (Fig. 4b and Table S2). The lower BE is typical of phosphorus in phosphine-like compounds [46] and is most probably from free (unreacted) PTA that is mixed with **3**. The doublet centred at higher BE is attributed to phosphorus from the complex, where the charged nitrogen atom, N⁺, seems to have an inducing effect on the phosphorus atom shifting its BE to higher values. N 1s regions before (in **3**) and after immobilization (in **3-AC**) were fitted with one main peak, centred at 399.8 ± 0.1 eV assigned to C-N, and another less intense peak attributed to quaternary nitrogen (N⁺), which is centred at 402.0 eV in the compound **3** and at slightly higher BE in **3-AC**, 402.8 eV (Fig. 4c and Table S2). When analysing the ratio N⁺/N, being N the non-charged nitrogen atoms, this ratio should be 0.5 in the complex, however the experimental ratio is

Table 2
Sn loading (wt%) on the carbon materials.^a

Carbon material	Sn(IV) complex	
	3	4
AC	2.1	1.83
AC-ox	2.65	2.37
AC-ox-Na	2.61	2.11
CNT	1.13	0.93
CNT-ox	1.48	1.27
CNT-ox-Na	1.40	1.32

^a Values obtained from ICP analysis.

much lower (Table S2), which means that indeed some free PTA may be mixed with the complex. Interestingly, this unreacted precursor seems to be absent in **3-AC**, as attested by the well-resolved P 2p doublet, with the main component detected at 132.8 eV assigned exclusively to the complex (Fig. 4b). The non-detection of the PTA-phosphine doublet after immobilization on AC, can be the result of free PTA entering the AC microporous structure, which could attenuate the XPS signal coming from buried moieties. Or, alternatively, if PTA gains a positive charge upon immobilization on AC, then its P 2p region must be coincident to the one from the complex. Regarding the tin XPS signal, the most intense orbital is the Sn 3d, which is a doublet of spin-orbit separation of 8.5 ± 0.1 eV (Fig. 4d). The photoelectron BE is not distinctive of the Sn oxidation state [46], however, in **3** the computed Auger Parameter (AP (Sn 3d_{5/2}, Sn N₄M₄₅M₄₅)) = 918.2 eV is closer to that of Sn(IV) species [47,48]. In **3-AC**, the Auger structure Sn MNN, needed to compute the AP, is not detected. Such effect can occur when the Auger electrons, which have lower kinetic energy than Sn 3d photoelectrons, are attenuated by an overlayer and cannot escape the surface [49]. This is compatible with tin being buried inside the AC porous surface. This effect can justify the Sn/P < 1 in **3-AC** (Table 3). On the other hand, for **3** this atomic ratio is larger than the predicted, showing that part of the Sn precursor did not react with the 4-(bromomethyl)benzoic acid. The Br 3d region which is also a doublet with energy separation of 1.1 eV and Br 3d_{5/2} centred at 68.1 eV is assigned to Br⁻ (Fig. 4e). Br⁻ is detected in compound **3**, with N⁺/Br⁻ = 1, but not in **3-AC**. This assignment excludes the presence of the precursor 4-(bromomethyl)benzoic acid or of compound **1**, since a bromine covalently bonded to carbon would have a Br 3d_{5/2} peak centred at BE higher than 70.5 eV [50].

2.3. Catalytic cyanosilylation of aldehydes

The catalytic efficiencies of the carbon-supported complexes **3** and **4** were evaluated in the cyanosilylation of aldehydes. The model experiment consisted in the addition reaction of benzaldehyde and TMSCN under microwave irradiation for rapid heating and in the absence of any solvent, which are favourable conditions for the development of sustainable reactions. The results are presented in Table 4.

The experiments were conducted at 50 °C, under low microwave irradiation (10 W), for 5 min, with 0.1 mol% catalyst loading and in solvent-free conditions (Table 4, entries 1–12). All the carbon-supported catalysts displayed catalytic activity towards the cyanosilylation of benzaldehyde, affording 2-phenyl-2-((trimethylsilyl)oxy)acetonitrile with no observed by-products, as confirmed by ¹H NMR. Complexes **3** and **4** on pristine supports, AC and CNT, showed superior catalytic activity with yields in the 72–94% range (Table 4, entries 1, 4, 7, and 10), compared to their chemically treated counterparts (Table 4, entries 2, 3, 5, 6, 8, 9, 11, 12). This difference in activity is likely due to the hydrophobic nature of the substrates making them more compatible with hydrophobic solid matrices (AC and CNT) as opposed to hydrophilic solid supports (the -ox and ox-Na analogues) that are introduced through surface modifications [51,52].

Catalysts based on AC supports (Table 4, entries 1 and 7) were found to be more active than those based on CNT (Table 4, entries 4 and 10). This can be attributed to the different characteristics of AC, such as microporosity and rich surface chemistry (as observed in the TPD profiles, Fig. S23), in comparison to CNT. Among the 12 carbon-supported Sn(IV) complexes tested as heterogeneous catalysts for the model reaction, **3-AC** exhibited the highest yield of the cyanohydrin product (94%, as shown in Table 4, entry 1), and the reaction conditions were further optimized to improve the yield.

A series of experiments were conducted to study the effect of temperature in the range from 30 to 60 °C (Table 4, entries 1 and 13–15). The results revealed that increasing the temperature to 50 °C improved the reaction rate, however, a further increase in temperature to 60 °C had a negative impact on the yield, likely caused by the partial thermal decomposition of the cyanohydrin product or the complex.

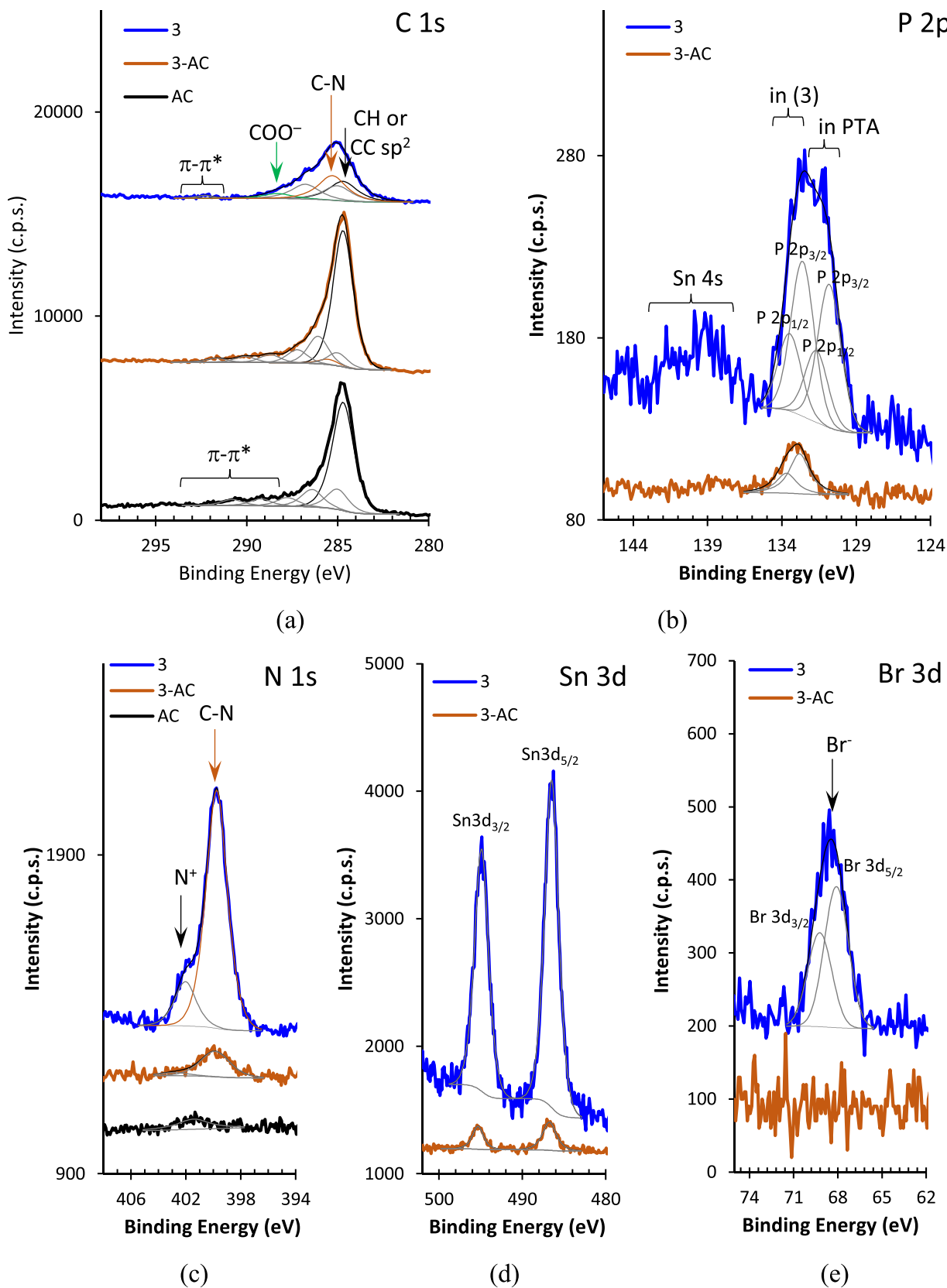


Fig. 4. XPS regions (a) C 1s, (b) P 2p, (c) N 1s, (d) Sn 3d and (e) Br 3d of samples AC (black), 3-AC (orange) and complex 3 (blue).

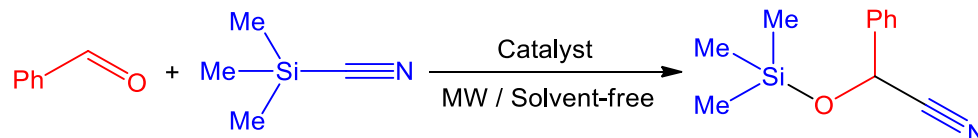
Table 3

XPS quantification: atomic concentrations (%) and relevant atomic ratios (n.d. – not detected).

	AC	3	3-AC	Predicted in (3)
C	89.9	70.4	89.9	68
O	9.5	13.3	8.7	8
N	0.5	9.3	0.95	12
P	—	2.4	0.24	4
Sn	—	3.1	0.19	4
Br	—	1.5	n.d.	4
Atomic ratios				
N/P	—	4.0	4.0	3
Sn/P	—	1.3	0.8	1
O/C	0.11	0.19	0.10	0.12

An extension of the reaction time to 10 min at 30 or 50 °C resulted in a considerable drop in the product yield from 86% and 94–76% and 78%, respectively (Table 4, entries 1 and 15–17). Furthermore, it was observed that increasing the catalyst amount from 0.1 to 0.2 mol% resulted in a decline of the yield from 94% to 79% (Table 4, entries 1 and 18).

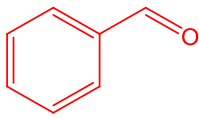
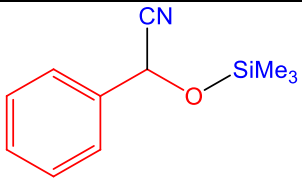
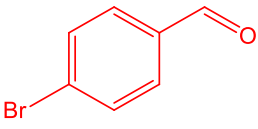
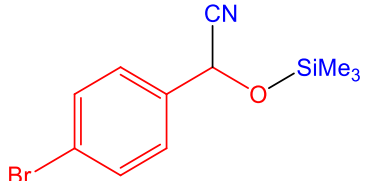
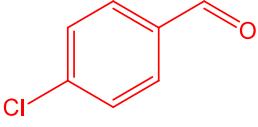
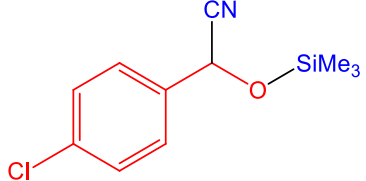
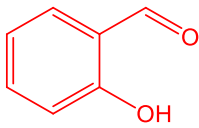
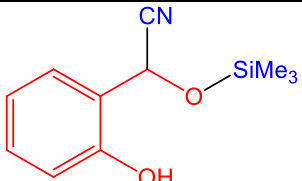
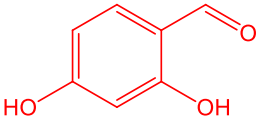
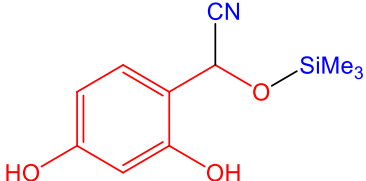
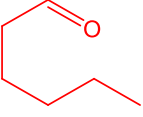
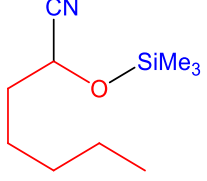
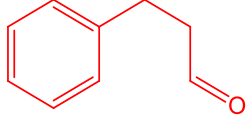
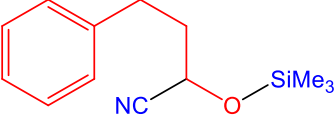
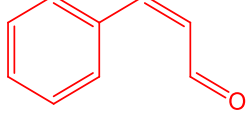
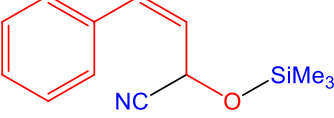
To understand the impact of the catalyst components on the reaction rate and to explore the possible mechanistic pathway, a series of experiments were performed using each component individually. Running blank reactions in the absence of the complex **3** and presence of the carbon materials afforded the product with yields up to only 18% (Table 4, entries 19–21). Using 1 mol% of Sn(IV) complex **1** as catalyst, which does not have the P moiety, led to an increase in the product yield to 30%, which demonstrates the role of the tin metal centre as a Lewis acid in activating the carbonyl group of the aldehyde (Table 4, entry 22).

Table 4Microwave-assisted cyanosilylation of benzaldehyde with TMSCN using carbon-supported tin complexes **3** and **4** as catalysts.^a


Entry	Catalyst	Catalyst Loading (mol%)	Time (min.)	Temperature (°C)	Yield ^b (%)	TON ^c
1	3-AC	0.1	5	50	94.3	943
2	3-AC-ox	0.1	5	50	12.0	120
3	3-AC-ox-Na	0.1	5	50	26.6	266
4	3-CNT	0.1	5	50	72.5	725
5	3-CNT-ox	0.1	5	50	30.5	305
6	3-CNT-ox-Na	0.1	5	50	27.8	278
7	4-AC	0.1	5	50	85.9	859
8	4-AC-ox	0.1	5	50	41.3	413
9	4-AC-ox-Na	0.1	5	50	49.6	496
10	4-CNT	0.1	5	50	82.7	827
11	4-CNT-ox	0.1	5	50	29.7	297
12	4-CNT-ox-Na	0.1	5	50	20.8	208
13	3-AC	0.1	5	60	81.0	810
14	3-AC	0.1	5	40	88.5	885
15	3-AC	0.1	5	30	86.0	860
16	3-AC	0.1	10	50	78.7	787
17	3-AC	0.1	10	30	76.3	763
18	3-AC	0.2	5	50	79.4	397
19	blank	-	5	50	10.7	-
20 ^d	AC	-	5	50	18.1	-
21 ^d	CNT	-	5	50	12.3	-
22	1	1.0	5	50	29.9	29.9
23 ^e	3	1.0	5	50	84.7	84.7
24	PTA	1.0	5	50	62.2	-
25 ^e	[PTA-CH ₂ -C ₆ H ₄ -p-COOH]Br	1.0	5	50	48.3	-

^a Reaction conditions: Benzaldehyde (25 mmol), TMSCN (26 mmol) and catalyst (0.1–1 mol% calculated based on the aldehyde).^b Determined by ¹H NMR analysis.^c Turnover number (number of moles of the product per mol of the metal catalyst).^d Reactions performed in the presence of 1 mg of the carbon material, without Sn catalyst.^e Reaction performed with free (not heterogenized) material, but not in homogeneous conditions, as these complexes are not soluble in the reaction media.

Table 5
Cyanosilylation of various aromatic and aliphatic aldehydes using 3-AC catalyst.^a

Entry	Aldehyde	Product	Yield ^b (%)	TON ^c
	$\text{R}-\text{CHO} + \text{Me}_3\text{Si}-\text{CN} \xrightarrow[\text{MW (10 W, 5 min, 50 }^\circ\text{C)}]{\text{3-AC (0.1 mol\%)}} \text{R}-\text{CH}(\text{CN})-\text{OSiMe}_3$			
1			>99	>990
2			>99	>990
3			85	850
4			75	750
5			28	280
6			>99	>990
7			>99	>990
8			75	750

^a Reaction conditions: aldehyde (1.0 mmol), TMSCN (1.2 mmol), 3-AC (0.1 mol%), 5 min, 50 °C, microwave (10 W).

^b Determined via ¹H NMR analysis. ^c Turnover number (moles of product per mole of catalyst).

Based on the results described in Table 4 (entries 22–24, and their above discussion), the mechanism of the reaction likely involves a double activation process through the Lewis acid and Lewis base sites of the supported complex **3**, specifically the Sn(IV) and the uncoordinated phosphorus centres, respectively. The reaction mechanism proceeds in a stepwise manner, starting with the interaction of the phosphorus and the silicon through the formation of a tetrel σ -hole bond $\text{NC}\cdots\text{Si}\cdots\text{P}$ in species **A** (Fig. 5). This enhances the nucleophilicity of the CN group by electron donation from Si. The formation of the tetrel σ -hole bond $\text{NC}\cdots\text{Si}\cdots\text{P}$ involves the interaction of the nucleophilic phosphorus with the positive region (σ -hole) at silicon atom on the opposite side of the strong electron acceptor cyano group. [54–57] The ^{29}Si NMR spectrum of an equimolar mixture of PTA and TMSiCN in $\text{DMSO-}d_6$ (Fig. S24) showed the resonance of TMSiCN at -11.21 ppm, and another peak at 7.34 ppm, which corresponds to the newly obtained PTA-TMS compound, thus providing evidence for the aforementioned tetrel σ -hole bond. Simultaneously, the Lewis acid Sn(IV) centre activates the carbonyl carbon of the aldehyde towards nucleophilic attack by the cyanide group, thus promoting cyanide transfer from silicon to the electrophilic carbonyl carbon and the $\text{Si}\cdots\text{O}$ interaction. The reaction possibly proceeds through a σ -bond metathesis with the formation of a four-membered transition state (species **B** in Fig. 5), ultimately leading to the cyanosilyl product liberation with catalyst regeneration.

The recyclability of the catalyst **3-AC** was assessed by conducting up to 4 consecutive cycles, as shown in Fig. 6. Each catalytic cycle was initiated by adding new portions of the reactants (benzaldehyde and TMSiCN) to the used catalyst, without any treatment. The reactions were performed using 0.1 mol% of the catalyst at 50°C under microwave irradiation for 5 min. Although a decrease in yield was observed per cycle, the catalyst still maintained a 72% yield after four consecutive runs. To determine whether the morphology of the carbon-supported catalyst had changed after recycling, the spent catalyst (after the fourth cycle) was examined by SEM. As shown in Fig. S25, the **3-AC** catalyst retained its structural features. The ICP analysis revealed that only a slight decrease in the metal amount ($<0.01\%$ Sn) was detected. This suggests that the **3-AC** catalytic system is a robust heterogeneous catalyst that does not allow metal leaching into the products.

The observed yield decrease after each cycle may be attributed to the poisoning of the active sites by trace impurities or adsorption of by-

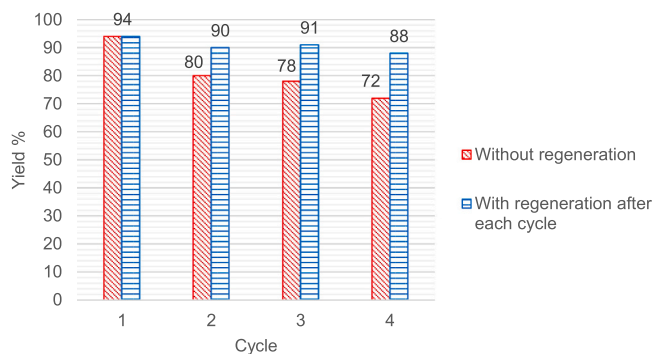


Fig. 6. Recycling studies using **3-AC** catalyst.

products on the catalyst surface, blocking the active sites. Therefore, we tried a different approach for recycling, which involves regenerating the catalyst after each cycle, aiming at removing of any organic reactants or impurities that may have accumulated on its surface. With this goal, after each cycle the catalyst was dispersed in hot acetone for three hours, then dried under vacuum at 50°C overnight (for a minimum of 12 h). The results showed that the regenerated catalyst maintained almost all its initial activity for at least four cycles, with the reaction yield remaining above 88% (Fig. 6).

3. Conclusions

In summary, this study presents the synthesis and characterization of new organotin compounds **3** and **4**, which contain the *N*-functionalized PTA ligand. These complexes were heterogenized on several carbon supports including commercially available (AC and CNT) and chemically modified (AC-ox, AC-ox-Na, CNT-ox and CNT-ox-Na) materials, and were used as catalysts for the cyanosilylation of aldehydes. The results showed that **3-AC** was the most active catalyst, obtaining cyanohydrins from several aldehyde substrates in excellent yields, after just 5 min at 50°C , under microwave irradiation and in solvent-free conditions, using only 0.1 mol% of the catalyst. The catalyst **3-AC** was also found to be recyclable, still maintaining a 88% yield of cyanohydrins

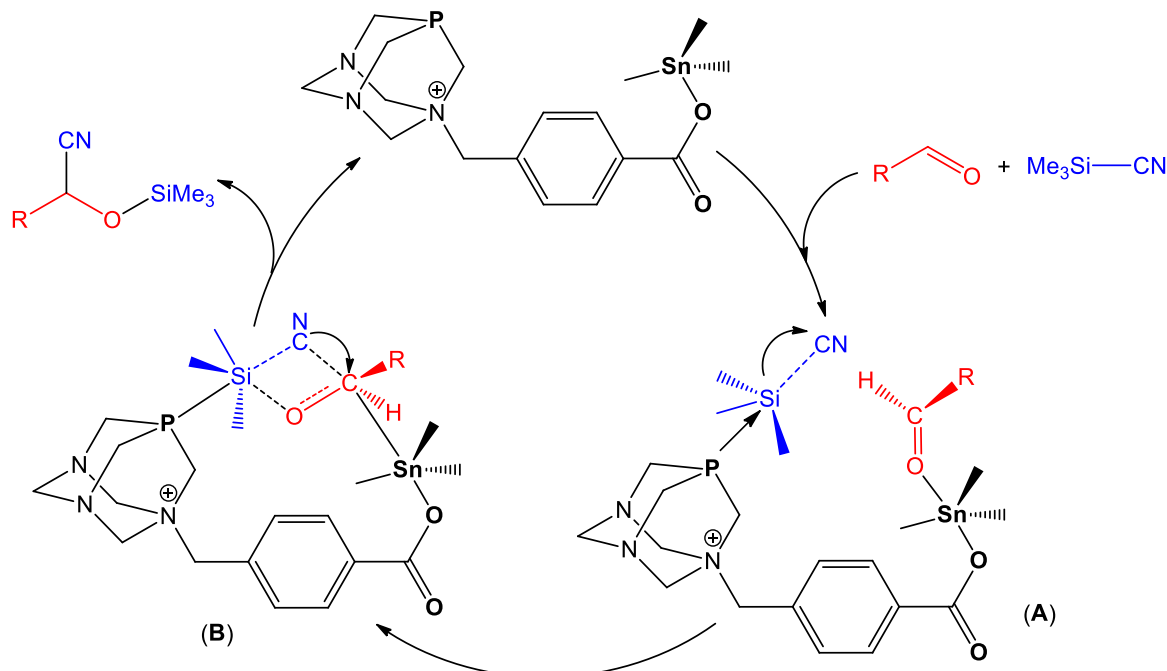


Fig. 5. Proposed mechanism for the cyanosilylation of aldehydes using **3** as a double-activation catalyst.

after four consecutive reaction cycles. In comparison with other heterogeneous metal-based catalysts for the cyanosilylation of aldehydes, **3-AC** was significantly more efficient in terms of high conversion, low reaction time and recyclability.

In situ multinuclear NMR investigations provided evidence for possible reaction intermediates and mechanistic pathways, suggesting that **3-AC** acts as a double activation catalyst through the Lewis acid and Lewis base sites. This study demonstrates the potential of these recyclable and efficient catalysts for the rapid cyanosilylation of aldehydes under mild and solvent-free conditions, which constitutes a step towards more “green” and scalable chemical transformations. The possibility of expanding the family of organotin complexes based on PTA derivatives, and the preparation of heterometallic compounds where the free P atom is coordinated to another soft metal centre, is currently being explored by the group.

4. Experimental

4.1. Materials and methods

The chemicals were obtained from commercial sources and were used without further purification. [PTA-CH₂-C₆H₄-p-COOH]Br was obtained according to the reported procedure [58]. Acetone was dried [59] prior to use as a solvent for the synthesis of **3** and **4**. IR spectra (4000–400 cm⁻¹) were obtained on a Vertex 70 (Bruker Corporation, Ettlingen, Germany) instrument in KBr pellets. Electrospray mass spectra were obtained with a Varian 500-MS LC Ion Trap Mass Spectrometer (Agilent Technologies, Santa Clara, CA, USA) equipped with an electrospray ion source. The Inductively Coupled Plasma (ICP) analyses were done at the Laboratório de Análises de Instituto Superior Técnico (IST). Carbon supports were degassed (150 °C) for 72 h prior to N₂ adsorption measurements at -196 °C using Micrometrics ASAP 2060 gas sorption instrument (Hidden Isochema, Warrington, UK). The surface characterization of supports was carried out in a previous work [41] by temperature-programmed desorption (TPD) using an Altamira AMI-300 apparatus with a coupled Ametek Dycor Dymaxion quadrupole mass spectrometer. The surface morphology of supports and immobilized complex **3** was determined by scanning electron microscopy (SEM) in a Hitachi S-2400 (Tokyo, Japan) instrument and transmission electron microscopy (TEM) in a Hitachi 8100 (Tokyo, Japan) equipment at IST MicroLab.

Multi-nuclear NMR spectra (¹H, ¹³C, ³¹P, ¹¹⁹Sn, ²⁹Si) were obtained from 300 MHz and 400 MHz spectrometers (Bruker Avance II, Bruker, Billerica, MA, USA) at ambient temperature. Chemical shifts δ are quoted in ppm, and coupling constants given in Hz. Multiplicities were abbreviated as follows: singlet (s), doublet (d) and multiplet (m). ¹H and ¹³C NMR spectra were internally referenced to residual protio-solvent resonance and are reported relative to tetramethylsilane ($\delta = 0$); ³¹P chemical shifts were referenced with external 85% H₃PO₄; ¹¹⁹Sn chemical shifts were referenced with external tetramethyltin. Assignments of some ¹H and ¹³C signals rely on g-COSY and g-HSQC experiments.

Syntheses under microwave irradiation were carried out in an Anton Paar Monowave 300 apparatus (Anton Paar GmbH, Graz, Austria). The reactions were performed in 4 mL cylindrical pyrex tubes, sealed using a teflon crimp top. After the reaction, the vial was cooled rapidly to ambient temperature by gas jet cooling.

X-ray Photoelectron Spectroscopy studies were conducted with a XSAM 800 dual anode spectrometer from KRATOS (Manchester, UK), using Mg K α X-rays with energy, $h\nu = 1253.6$ eV. Operational and acquisition conditions, and data treatment details were described elsewhere [48]. The charge shift was corrected using as reference the binding energy (BE) of aromatic carbon atoms, set at 284.7 eV. The sensitivity factors of the spectrometer software library (Vision 2 for Windows, Version 2.2.9 - KRATOS) were used for quantitative analysis.

4.2. Synthesis of the compounds 1–4

4.2.1. [(BrCH₂-C₆H₄-p-COO)SnR₃] (R = Me for **1** and Ph for **2**)

In a 250 mL round-bottomed flask equipped with a Dean-Stark apparatus and a condenser, a mixture of 4-(bromomethyl)benzoic acid (0.93 mmol, 0.2 g), (CH₃)₃SnOH (0.93 mmol, 0.17 g) for compound **1** or Ph₃SnOH (0.93 mmol, 0.34 g) for compound **2**, and toluene (60 mL) was stirred and heated under reflux for 5 h. The resulting clear and colourless solution was cooled and the solvent was reduced to approximately 5 mL. The product was obtained after adding petroleum ether (30–40 mL) and isolated as a white solid after filtration and drying under vacuum.

Compound 1. Yield: 80% based on metal salt. Elemental analysis calcd (%) for C₁₁H₁₅BrO₂Sn: C 34.97, H 4.00; found: C 34.71, H 4.13. FTIR (KBr, cm⁻¹): 2643 (br), 1598 (s), 1559 (s), 1370 (s), 1228 (s), 781 (s), 552 (s). ¹H NMR (δ , 300 MHz; DMSO-*d*₆): 7.84 (d, *J* = 7.5 Hz, 2 H, Ar-H), 7.46 (d, *J* = 7.8 Hz, 2 H, Ar-H), 4.72 (s, 2 H, CH₂), 0.48 (s, 9 H, CH₃). ¹¹⁹Sn{¹H} NMR (δ , 300 MHz; DMSO-*d*₆): -15.31. The NMR spectra can be found in Figs. S1 and S2 and the FTIR spectra in Fig. S19.

Compound 2. Yield: 74% based on metal salt. Elemental analysis calcd (%) for C₂₆H₂₁BrO₂Sn: C 55.36, H 3.75; found: C 55.17, H 3.90. FTIR (KBr, cm⁻¹): 3054 (s), 1627 (s), 1429 (s), 1291 (s), 704 (s), 602 (s). ¹H NMR (δ , 400 MHz; DMSO-*d*₆): 7.97–7.76 (m, 8 H, Ar-H), 7.47–7.40 (m, 11 H, Ar-H), 4.69 (s, 2 H, CH₂). ¹³C{¹H} NMR (δ , 400 MHz; DMSO-*d*₆) /DEPT/HSQC: 143.70 (C{O}), 143.11 (Ar-C_{quad}-CH₂), 136.24 (Ar-C_{quad}-Sn), 136.01 (Ar-CHCSn), 132.53 (Ar-CHCHCSn), 129.66 (Ar-CHCHCHCSn), 129.14 (Ar-CHCC{O}), 128.51 (Ar-CHCCH₂), 128.38 (Ar-C_{quad}-C{O}). ¹¹⁹Sn{¹H} NMR (δ , 300 MHz; DMSO-*d*₆): -230.52. The NMR spectra can be found in Figs. S3 and S4 and the FTIR spectra in Fig. S20.

4.2.2. [(PTA-CH₂-C₆H₄-p-COO)SnR₃]Br (R = Me for **3** and Ph for **4**)

To an acetone solution (20 mL) of compound **1** (0.13 mmol, 49 mg; to obtain complex **3**) or compound **2** (0.13 mmol, 76 mg; to obtain complex **4**), a solution of PTA (0.13 mmol, 22 mg) in acetone (10 mL) was added dropwise under a nitrogen atmosphere and with vigorous stirring at room temperature. The mixture was stirred for 3 h, after which the white solid products were isolated by filtration, washed with acetone and dried under vacuum.

Compound 3. Yield: 88% based on PTA. Elemental analysis calcd (%) for C₁₇H₂₇BrN₃O₂PSn: C 38.17, H 5.09, N 7.85; found: C 38.35, H 5.18, N 7.90. FTIR (KBr, cm⁻¹): 3417 (br), 2987 (b), 1657 (s), 1567 (s), 1372 (s), 1125 (s), 1033 (s), 782 (s), 550 (s). ¹H NMR (δ , 400 MHz; DMSO-*d*₆): 7.95 (d, *J* = 7.2 Hz, 2 H, Ar-H), 7.52 (d, *J* = 7.6 Hz, 2 H, Ar-H), 5.08 (d, *J* = 10.8 Hz, 2 H, N⁺CH₂N), 4.86 (d, *J* = 11.2 Hz, 2 H, N⁺CH₂N), 4.53 (d, *J* = 13.6 Hz, 1 H, NCH₂N), 4.36 (d, *J* = 13.2 Hz, 1 H, NCH₂N), 4.24 (d, *J* = 4.8 Hz, 2 H, PCH₂N⁺), 4.17 (s, 2 H, CCH₂N⁺), 3.94–3.75 (m, 4 H, PCH₂N), 0.49 (s, 9 H, CH₃). ³¹P{¹H} NMR (δ , 400 MHz; DMSO-*d*₆): -83.63. ¹³C{¹H} NMR (δ , 300 MHz; DMSO-*d*₆): 168.69 (C{O}), 132.67 (Ar-CH), 129.65 (Ar-CH), 78.71 (NCH₂N⁺), 69.31 (NCH₂N), 64.25 (CCH₂N⁺), 51.62 (¹J_{pc} = 130.4 Hz, PCH₂N⁺), 45.27 (¹J_{pc} = 81.6 Hz, PCH₂N), 0.76 (SiCH₃). DEPT (δ , 300 MHz; DMSO-*d*₆): 132.42, 129.40, 78.45, 69.05, 63.99, 51.36, 45.10, 0.51. ¹¹⁹Sn{¹H} NMR (δ , 300 MHz; DMSO-*d*₆): -19.65. ESI(+)/MS in DMSO (*m/z*): 455.9 (calcd. 455.1) [(PTA-CH₂-C₆H₄-p-COO)SnMe₃]⁺. The NMR spectra can be found in Figs. S5 and S11.

Compound 4. Yield: 48% based on PTA. Elemental analysis calcd (%) for C₃₂H₃₃BrN₃O₂PSn: C 53.29, H 4.61, N 5.83; found: C 52.95, H 4.57, N 5.65. FTIR (KBr, cm⁻¹): 3413 (br), 1625 (s), 1354 (s), 1125 (s), 1070 (s), 1034 (s), 816 (s), 736 (s), 700 (s), 555 (m). ¹H NMR (δ , 400 MHz; DMSO-*d*₆)/COSY: 7.99 (m, 7 H, Ar-H), 7.95 (d, *J* = 7.6 Hz, 2 H, Ar-H), 7.49 (d, *J* = 7.6 Hz, 2 H, Ar-H), 7.32 (m, 8 H, Ar-H), 5.08 (d, *J* = 10.8 Hz, 2 H, N⁺CH₂N), 4.86 (d, *J* = 10.8 Hz, 2 H, N⁺CH₂N), 4.53 (d, *J* = 13.2 Hz, 1 H, NCH₂N), 4.36 (d, *J* = 13.2 Hz, 1 H, NCH₂N), 4.24

(d, $J = 3.5$ Hz, 2 H, PCH_2N^+), 4.14 (s, 2 H, CCH_2N^+), 3.90–3.75 (m, 4 H, PCH_2N). $^{31}\text{P}\{^1\text{H}\}$ NMR (δ , 400 MHz; DMSO- d_6): – 83.72. $^{13}\text{C}\{^1\text{H}\}$ NMR (δ , 400 MHz; DMSO- d_6)/DEPT/HSQC: 168.04 (C{O}), 146.65 (Ar- $\text{C}_{\text{quad}}\text{-CH}_2$), 138.34 (Ar- $\text{C}_{\text{quad}}\text{-Sn}$), 136.41 (Ar-CHCSn), 132.53 (Ar-CHCHCSn), 129.57 (Ar-CHCHCHCSn), 127.99 (Ar-CHCC{O}), 127.67 (Ar-CHCCH $_2$), 127.31 (Ar- $\text{C}_{\text{quad}}\text{-C}\{O\}$), 78.70 (NCH_2N^+), 69.32 (NCH_2N), 64.34 (CCH_2N^+), 51.61 ($^1J_{\text{PC}} = 130$ Hz, PCH_2N^+), 45.37 ($^1J_{\text{PC}} = 84.2$ Hz, PCH_2N). DEPT (δ , 400 MHz; DMSO- d_6): 136.16, 132.28, 129.32, 127.75, 127.42, 78.44, 69.07, 64.08, 51.35, 45.06. $^{119}\text{Sn}\{^1\text{H}\}$ NMR (δ , 300 MHz; DMSO- d_6): – 326.43. ESI(+)-MS (m/z): 642.02 (calcd. 641.32) [(PTA- $\text{CH}_2\text{-C}_6\text{H}_4\text{-p-COO}\text{)SnPh}_3]^+$. The NMR spectra can be found in Figs. S12 and S18.

4.3. Preparation of the supported catalysts

4.3.1. Treatment of the carbon materials

The activated carbon (AC) and multi-walled carbon nanotubes (CNT) were used as solid supports. The AC-ox and CNT-ox supports were obtained from refluxing 1 g of carbon in 5 M HNO_3 (75 mL) solution for 3 h, followed by filtration and washing with distilled water until neutral pH. [44,60] The AC-ox-Na and CNT-ox-Na materials were attained from the 1 h reflux of AC-ox and CNT-ox with 20 mM NaOH (75 mL) solution, followed by filtration and washing with distilled water until neutral pH, respectively. [44,60].

4.3.2. Immobilization of the complexes

The carbon material (150 mg) was added to an aqueous solution of the complex (50 mg) dissolved in 50 mL of water. The obtained mixture was stirred at room temperature for 72 h. The carbon-supported materials were separated by filtration, washed with water and dried under vacuum, at 120 °C for 24 h. The metal (Sn) loading was determined by ICP.

4.4. General procedure for cyanosilylation of aldehydes

In a typical experiment, a 4 mL microwave tube was used, which was equipped with a magnetic stirring bar. The tube contained a 25 mmol of aldehyde, 26 mmol of trimethylsilyl cyanide (TMSCN), and a carbon-supported catalyst. The mixture was placed in a microwave reactor and stirred at 600 RPM while being heated at 10 W for 5 min at 50 °C. After the reaction, the mixture was centrifuged to separate the heterogenized catalyst. The desired product was then quantified by diluting the mixture with CDCl_3 and analysing it using ^1H NMR.

For the regeneration process, the catalyst was dispersed in acetone at 50 °C for 3 h. After filtering off, the catalyst was dried under vacuum at 50 °C overnight (for at least 12 h) before being used for the next catalytic cycle.

CRediT authorship contribution statement

Abdallah G. Mahmoud: Conceptualization, Validation, Investigation, Data Curation, Writing – original draft; **Ivy L. Librando:** Writing – Original Draft, Methodology, Formal analysis, Investigation, Visualization. **Anup Paul:** Conceptualization, Methodology, Validation, Formal analysis, Investigation, Supervision, Project administration, Writing – review & editing. **Sônia A. C. Carabineiro:** Conceptualization, Methodology, Validation, Investigation; supervision, Writing – review & editing. **Ana Maria Ferraria:** Formal analysis; Investigation; Writing – original draft, Writing – review & editing, Visualization. **Ana Maria Botelho do Rego:** Writing – review & editing. **M. Fátima C. Guedes da Silva:** Conceptualization, Supervision, Resources, validation, visualization, writing; reviewing and editing; **Carlos F.G.C. Geraldes:** Supervision, Writing – review & editing. **Armando J.L. Pombeiro:** Resources, Validation, Visualization, Project administration, Funding acquisition, Writing – review & editing; All authors read and approved the final manuscript and agreed with its contents and publication in the final

form.

Declaration of Competing Interest

The authors declare that they have no known competing financial interests or personal relationships that could have appeared to influence the work reported in this paper.

Data Availability

Data will be made available on request.

Acknowledgements and Funding

The authors are grateful for the financial support from Fundação para a Ciência e a Tecnologia (FCT), Portugal, through projects UIDB/00100/2020, UIDP/00100/2020 and LA/P/0056/2020 of Centro de Química Estrutural; projects UIDB/04565/2020, UIDP/04565/2020, and LA/P/0140/2020 of Institute for Bioengineering and Biosciences – iBB and the Associate Laboratory Institute for Health and Bioeconomy – i4HB and projects UIDB/50020/2020 and UIDP/50020/2020 (LSRE-LCM). The work was also funded by national funds through FCT, under the Scientific Employment Stimulus-Institutional Call (CEEC-INST/00102/2018). We also acknowledge the Associate Laboratory for Green Chemistry – LAQV financed by national funds from FCT/MCTES (UIDB/50006/2020 and UIDP/5006/2020) and Base-UIDB/50020/2020 and Programmatic UIDP/50020/2020 funding of the Associate Laboratory LSRE-LCM. AGM is grateful to Associação do Instituto Superior Técnico para a Investigação e Desenvolvimento (IST-ID) for his post-doctoral fellowship through grant no. BL133/2021-IST-ID. ILL acknowledges the CATSUS PhD Program from FCT for her grant PD/BD/135555/2018. AP and AMF are grateful to FCT and Instituto Superior Técnico (IST), Portugal through DL/57/2017 (Contract no. IST-ID/197/2019 and IST-ID/131/2018). This publication is also supported by the RUDN University Strategic Academic Leadership Program (recipient AJLP, preparation). The authors also acknowledge the Portuguese NMR Network (IST-UL Centre) for access to the NMR facility. CFGCG thanks the FCT for funding of CQC-IMS through the projects UIDB/00313/2020 and UIDP/00313/2020.

Appendix A. Supporting information

Supplementary data associated with this article can be found in the online version at doi:10.1016/j.cattod.2023.114270.

References

- [1] R.J.H. Gregory, Cyanohydrins in nature and the laboratory: biology, preparations, and synthetic applications, *Chem. Rev.* 99 (1999) 3649–3682, <https://doi.org/10.1021/CR9902906>.
- [2] C.J. Peterson, R. Tsao, J.R. Coats, Naturally occurring cyanohydrins, analogues and derivatives as potential insecticides, *Pest Manag. Sci.* 56 (2000) 615–617, [https://doi.org/10.1002/1526-4998\(200007\)56:7<615::AID-PS173>3.0.CO;2-W](https://doi.org/10.1002/1526-4998(200007)56:7<615::AID-PS173>3.0.CO;2-W).
- [3] J. Tao, G.-Q. Lin, A. Liese, eds., *Biocatalysis for the Pharmaceutical Industry: Discovery, Development, and Manufacturing*, John Wiley & Sons, 2009.
- [4] J.-M. Brunel, I.P. Holmes, I.P. Holmes, J.-M. Brunel, Chemically catalyzed asymmetric cyanohydrin syntheses, *Angew. Chem. Int. Ed.* 43 (2004) 2752–2778, <https://doi.org/10.1002/ANIE.200300604>.
- [5] M. North, D.L. Usanov, C. Young, Lewis acid catalyzed asymmetric cyanohydrin synthesis, *Chem. Rev.* 108 (2008) 5146–5226, <https://doi.org/10.1021/CR800255K>.
- [6] A.G. Mahmoud, K.T. Mahmudov, M.F.C. Guedes da Silva, A.J.L. Pombeiro, Reaction of sodium 2-(2-(2,4-dioxopent-3-ylidene)hydrazinyl) benzenesulfonate with ethylenediamine on Cu(II) and Ni(II) centres: efficient Cu(II) homogeneous catalysts for cyanosilylation of aldehydes, *RSC Adv.* 6 (2016) 54263–54269, <https://doi.org/10.1039/C6RA12274D>.
- [7] A.V. Gurbanov, A.M. Maharramov, M.F.C. Guedes da Silva, A.J.L. Pombeiro, Trinuclear and polymeric cobalt(II or III) complexes with an arylhydrazone of acetoacetanilide and their application in cyanosilylation of aldehydes, *Inorg. Chim. Acta* 466 (2017) 632–637, <https://doi.org/10.1016/J.ICA.2017.07.004>.
- [8] A.V. Gurbanov, G. Mahmoudi, M.F.C. Guedes da Silva, F.I. Zubkov, K. T. Mahmudov, A.J.L. Pombeiro, Cyanosilylation of aldehydes catalyzed by mixed

- ligand copper(II) complexes, *Inorg. Chim. Acta* 471 (2018) 130–136, <https://doi.org/10.1016/J.ICA.2017.10.042>.
- [9] S. Pahar, G. Kundu, S.S. Sen, Cyanosilylation by compounds with main-group elements: an odyssey, *ACS Omega* 5 (2020) 25477–25484, <https://doi.org/10.1021/acsomega.0c03293>.
- [10] C. Baleizão, B. Gigante, H. Garcia, A. Corma, Vanadyl salen complexes covalently anchored to single-wall carbon nanotubes as heterogeneous catalysts for the cyanosilylation of aldehydes, *J. Catal.* 221 (2004) 77–84, <https://doi.org/10.1016/j.jcat.2003.08.016>.
- [11] C. Baleizão, B. Gigante, H. García, A. Corma, Chiral vanadyl salen complex anchored on supports as recoverable catalysts for the enantioselective cyanosilylation of aldehydes. Comparison among silica, single wall carbon nanotube, activated carbon and imidazolium ion as support, *Tetrahedron* 60 (2004) 10461–10468, <https://doi.org/10.1016/j.tet.2004.08.077>.
- [12] W.T. Piver, Organotin compounds: industrial applications and biological investigation, *Environ. Health Perspect.* 4 (1973) 61–79, <https://doi.org/10.1289/ehp.730461>.
- [13] A. Mohammed, G.A. El-Hiti, E. Yousif, A.A. Ahmed, D.S. Ahmed, M.H. Alotaibi, Protection of poly(vinyl chloride) films against photodegradation using various valsartan tin complexes, *Polymers* 12 (2020) 969, <https://doi.org/10.3390/polym12040969>.
- [14] B. Watheq, E. Yousif, M.H. Al-Mashhadani, A. Mohammed, D.S. Ahmed, M. Kadhom, A.H. Jawad, A surface morphological study, poly(vinyl chloride) photo-stabilizers utilizing ibuprofen tin complexes against ultraviolet radiation, *Surfaces* 3 (2020) 579–593, <https://doi.org/10.3390/surfaces3040039>.
- [15] A.B. Ferreira, A. Lemos Cardoso, M.J. da Silva, Tin-catalyzed esterification and transesterification reactions: a review, *ISRN Renew. Energy* 2012 (2012) 1–13, <https://doi.org/10.5402/2012/142857>.
- [16] A.V. Gurbanov, F.E. Huseynov, A.M. Maharramov, M.F.C. Guedes da Silva, A.J.L. Pombeiro, Cyanosilylation of aldehydes catalyzed by arylhydrazine di- and triorganotin(IV) complexes, *J. Organomet. Chem.* 848 (2017) 118–121, <https://doi.org/10.1016/J.JORGANOCHEM.2017.07.030>.
- [17] L.M.D.R.S. Martins, S. Hazra, M.F.C. Guedes da Silva, A.J.L. Pombeiro, A sulfonated Schiff base dimethyltin(IV) coordination polymer: synthesis, characterization and application as a catalyst for ultrasound- or microwave-assisted Baeyer–Villiger oxidation under solvent-free conditions, *RSC Adv.* 6 (2016) 78225–78233, <https://doi.org/10.1039/C6RA14689A>.
- [18] S. Hazra, N.M.R. Martins, M.L. Kuznetsov, M.F.C. Guedes da Silva, A.J.L. Pombeiro, Flexibility and lability of a phenyl ligand in hetero-organometallic 3d metal–Sn(IV) compounds and their catalytic activity in Baeyer–Villiger oxidation of cyclohexanone, *Dalton Trans.* 46 (2017) 13364–13375, <https://doi.org/10.1039/C7DT02534C>.
- [19] M. Kaur, A. Kapila, V. Yempally, H. Kaur, Synthesis, structural elucidation, and catalytic activity of bimetallic rhenium-tin complexes containing Schiff base ligand, *J. Mol. Struct.* 1249 (2022), 131545, <https://doi.org/10.1016/j.molstruc.2021.131545>.
- [20] A. Karmakar, S. Hazra, G.M.D.M. Rúbio, M.F.C. Guedes da Silva, A.J.L. Pombeiro, Packing polymorphism in 3-amino-2-pyrazinylcarboxylate based tin(II) complexes and their catalytic activity towards cyanosilylation of aldehydes, *New J. Chem.* 42 (2018) 17513–17523, <https://doi.org/10.1039/C8NJ03805H>.
- [21] K. Sheng, L.M. Fan, X.F. Tian, R.K. Gupta, L. Gao, C.H. Tung, D. Sun, Temperature-induced Sn(II) supramolecular isomeric frameworks as promising heterogeneous catalysts for cyanosilylation of aldehydes, *Sci. China Chem.* 63 (2020) 182–186, <https://doi.org/10.1007/s11426-019-9621-x>.
- [22] A.D. Phillips, L. Gonsalvi, A. Romerosa, F. Vizza, M. Peruzzini, Coordination chemistry of 1,3,5-triaza-7-phosphaadamantane (PTA): Transition metal complexes and related catalytic, medicinal and photoluminescent applications, *Coord. Chem. Rev.* 248 (2004) 955–993, <https://doi.org/10.1016/J.CCR.2004.03.010>.
- [23] A. Guerriero, M. Peruzzini, L. Gonsalvi, Coordination chemistry of 1,3,5-triaza-7-phosphatricyclo[3.3.1.1]decane (PTA) and derivatives. Part III. Variations on a theme: Novel architectures, materials and applications, *Coord. Chem. Rev.* 355 (2018) 328–361, <https://doi.org/10.1016/J.CCR.2017.09.024>.
- [24] A.G. Mahmoud, M.F.C. Guedes da Silva, A.J.L. Pombeiro, 3,7-Diacetyl-1,3,7-triaza-5-phospha-bicyclo[3.3.1]nonane (DAPTA) and derivatives: coordination chemistry and applications, *Coord. Chem. Rev.* 429 (2021), 213614, <https://doi.org/10.1016/j.ccr.2020.213614>.
- [25] F. Scalambra, P. Lorenzo-Luis, I.D.L. Ríos, A. Romerosa, New findings in metal complexes with antiproliferative activity containing 1, 3, 5-Triaza-7-phosphaadamantane (PTA) and derivative ligands, *Eur. J. Inorg. Chem.* 2019 (2019) 1529–1538, <https://doi.org/10.1002/ejic.201801426>.
- [26] A.G. Mahmoud, M.F.C. Guedes da Silva, P. Smoleński, Insights into copper complexes of PTA and related ligands: synthesis, structural features and applications, in: A.J.L. Pombeiro (Ed.), *Synth. AndCatalysis Sustain.*, World Scientific Publishing Company, 2024, pp. 77–106, https://doi.org/10.1142/9789811279942_0003.
- [27] A.G. Mahmoud, M.F.C. Guedes da Silva, J. Sokolnicki, P. Smoleński, A.J.L. Pombeiro, Hydro-soluble Cu(I)-DAPTA complexes: synthesis, characterization, luminescence thermochromism and catalytic activity for microwave-assisted three-component azide-alkyne cycloaddition click reaction, *Dalton Trans.* 47 (2018) 7290–7299, <https://doi.org/10.1039/C8DT01232F>.
- [28] A.G. Mahmoud, M.F.C. Guedes da Silva, E.I. Śliwa, P. Smoleński, M.L. Kuznetsov, A.J.L. Pombeiro, Copper(II) and Sodium(II) Complexes based on 3,7-Diacetyl-1,3,7-triaza-5-phospha-bicyclo[3.3.1]nonane-5-oxide: Synthesis, Characterization, and Catalytic Activity, *Chem. Asian J.* 13 (2018) 2868–2880, <https://doi.org/10.1002/ASIA.201800799>.
- [29] A.G. Mahmoud, P. Smoleński, M.F.C. Guedes da Silva, A.J.L. Pombeiro, Molecules Water-Soluble O-, S-and Se-Functionalized Cyclic Acetyl-triaza-phosphines. Synthesis, characterization and application in catalytic azide-alkyne cycloaddition, *Molecules* 25 (2020) 5479, <https://doi.org/10.3390/molecules25255479>.
- [30] A.G. Mahmoud, M.F.C. Guedes da Silva, A.J.L. Pombeiro, A new amido-phosphane as ligand for copper and silver complexes. Synthesis, characterization and catalytic application for azide-alkyne cycloaddition in glycerol, *Dalton Trans.* 50 (2021) 6109–6125, <https://doi.org/10.1039/d1dt00992c>.
- [31] I.L. Librando, A.G. Mahmoud, S.A.C. Carabineiro, M.F.C. Guedes da Silva, C.F.G. C. Geraldes, A.J.L. Pombeiro, The catalytic activity of carbon-supported Cu(I)-phosphine complexes for the microwave-assisted synthesis of 1,2,3-triazoles, *Catalysts* 11 (2021) 185, <https://doi.org/10.3390/catal11020185>.
- [32] I.L. Librando, A.G. Mahmoud, S.A.C. Carabineiro, M.F.C. Guedes da Silva, C.F.G. C. Geraldes, A.J.L. Pombeiro, Synthesis of a novel series of Cu(I) complexes bearing alkylated 1,3,5-triaza-7-phosphaadamantane as homogeneous and carbon-supported catalysts for the synthesis of 1- and 2-substituted-1,2,3-triazoles, *Nanomaterials* 11 (2021) 2702, <https://doi.org/10.3390/NANO11102702>.
- [33] I.L. Librando, A. Paul, A.G. Mahmoud, A.V. Gurbanov, S.A.C. Carabineiro, F. C. Guedes da Silva, C.F.G.C. Geraldes, A.J.L. Pombeiro, Triazaphosphaadamantane-functionalized terpyridine metal complexes: cyclohexane oxidation in homogeneous and carbon-supported catalysis, *RSC Sustain.* 1 (2023) 147–158, <https://doi.org/10.1039/D2SU00017B>.
- [34] T.S. Basu Baul, A. Paul, L. Pellerito, M. Scopelliti, P. Singh, P. Verma, D. De Vos, Triphenyltin(IV) 2-[(E)-2-(aryl)-1-diazenyl]benzoates as anticancer drugs: synthesis, structural characterization, in vitro cytotoxicity and study of its influence towards the mechanistic role of some key enzymes *Invest. N. Drugs* 28 (2010) 587–599 doi: 10.1007/S10637-009-9293-X/FIGURES/9.
- [35] T.S. Basu Baul, A. Paul, L. Pellerito, M. Scopelliti, A. Duthie, D. De Vos, R.P. Verma, U. Englert An in vitro comparative assessment with a series of new triphenyltin(IV) 2-/4-[(E)-2-(aryl)-1-diazenyl]benzoates endowed with anticancer activities: Structural modifications, analysis of efficacy and cytotoxicity involving human tumor cell lines *J. Inorg. Biochem.* 107 (2012) 119–128 doi: 10.1016/J.JINORGBIO.2011.10.008.
- [36] T.S. Basu Baul, A. Chaurasiya, A. Duthie, P. Montes-Tolentino, H. Höpfl, Coordination-driven self-assembly of macrocycles and 1D or 2D coordination polymers using heteroditopic pyridyl-carboxylate ligands: the case study of 5-[(E)-2-(3-Pyridyl)-1-diazenyl]-2-hydroxybenzoate in combination with [RnSn] (n = 2 and 3) Cryst. Growth Des. 19 (2019) 6656–6671 doi: 10.1021/ACS.CGD.9B01045.
- [37] I. Ahmad, A. Zia-ur-Rehman, M. Waseem, C. Tariq, J. MacBeth, D. Bacsa, A. Venkataraman, N. Rajakumar, S. Ullah, Tabassum, Organotin(IV) derivatives of amide-based carboxylates: Synthesis, spectroscopic characterization, single crystal studies and antimicrobial, antioxidant, cytotoxic, anti-leishmanial, hemolytic, noncancerous, anticancer activities, *Inorg. Chim. Acta* 505 (2020), 119433, <https://doi.org/10.1016/J.ICA.2020.119433>.
- [38] M. Sirajuddin, S. Ali, V. McKee, A. Wadood, M. Ghufuran, Exploration of organotin (IV) derivatives for medicinal applications: Synthesis, spectroscopic characterization, structural elucidation and molecular docking study, *J. Mol. Struct.* 1181 (2019) 93–108, <https://doi.org/10.1016/J.MOLSTRUC.2018.12.041>.
- [39] F. Shaheen, M. Sirajuddin, S. Ali, N.A. Shah, B. Kanwal, M.N. Tahir, New tri- and di-alkylstannyl 2-(1H-indol-3-yl)ethanoates: synthesis, characterization and biological screenings, *J. Coord. Chem.* 73 (2020) 934–946, <https://doi.org/10.1080/00958972.2020.1749272>.
- [40] V.K. Choudhary, A.K. Bhatt, N. Sharma, Theoretical and spectroscopic evidence on a new triphenyltin(IV) 3,5-dinitrosalicylhydroxamate complex: synthesis, structural characterization, and biological screening, *J. Coord. Chem.* 73 (2020) 947–968, <https://doi.org/10.1080/00958972.2020.1747055>.
- [41] M. Sutradhar, L.M.D.R.S. Martins, S.A.C. Carabineiro, M.F.C. Guedes da Silva, J. G. Buijnsters, J.L. Figueiredo, A.J.L. Pombeiro, Oxidovanadium(V) complexes anchored on carbon materials as catalysts for the oxidation of 1-phenylethanol, *ChemCatChem* 8 (2016) 2254–2266, <https://doi.org/10.1002/cctc.201600316>.
- [42] M. Jaroniec, J. Choma, Characterization of nanoporous carbons by using gas adsorption Isotherms, in: T.J. Bandosz (Ed.), *Act. Carbon Surfaces Environ. Remediat., first ed.*, Elsevier, 2006, pp. 107–158.
- [43] A.P.C. Ribeiro, I.A.S. Matias, S.A.C. Carabineiro, L.M.D.R.S. Martins, Commercial gold complexes supported on functionalised carbon materials as efficient catalysts for the direct oxidation of ethane to acetic acid, *Page 165.* 12, *Catalysis Vol.* 12 (2022) 165, <https://doi.org/10.3390/CATAL12020165>.
- [44] S.A.C. Carabineiro, L.M.D.R.S. Martins, A.J.L. Pombeiro, J.L. Figueiredo, Commercial Gold(I) and Gold(III) compounds supported on carbon materials as greener catalysts for the oxidation of alkanes and alcohols, *ChemCatChem* 10 (2018) 1804–1813, <https://doi.org/10.1002/cctc.201701886>.
- [45] D. Tsyganov, N. Bundaleska, A. Dias, J. Henriques, E. Felizardo, M. Abrashev, J. Kissovski, A.M.B. Do Rego, A.M. Ferraria, E. Tatarova, Microwave plasma-based direct synthesis of free-standing N-graphene, *Phys. Chem. Chem. Phys.* 22 (2020) 4772–4787, <https://doi.org/10.1039/C9CP05509F>.
- [46] A.V. Naumkin, A. Kraut-Vass, S.W. Gaarenstroom, C.J. Powell, NIST X-ray photoelectron spectroscopy (XPS) database, NIST Stand. Ref. Database 20 4 (2012) 1, <https://doi.org/10.18434/T4T88K>.
- [47] V.M. Jiménez, J.A. Mejías, J.P. Espinós, A.R. González-Elipse, Interface effects for metal oxide thin films deposited on another metal oxide II. SnO₂ deposited on SiO₂, *Surf. Sci.* 366 (1996) 545–555, [https://doi.org/10.1016/0039-6028\(96\)00831-X](https://doi.org/10.1016/0039-6028(96)00831-X).
- [48] S. Salomé, A.M. Ferraria, A.M. Botelho Do Rego, F. Alcaide, O. Savadogo, R. Rego, Enhanced activity and durability of novel activated carbon-supported PdSn heat-treated cathode catalyst for polymer electrolyte fuel cells, *Electrochim. Acta* 192 (2016) 268–282, <https://doi.org/10.1016/J.ELECTACTA.2016.01.177>.

- [49] R. Rego, A.M. Ferraria, A.M. Botelho Do Rego, M.C. Oliveira, Development of PdP nano electrocatalysts for oxygen reduction reaction, *Electrochim. Acta* 87 (2013) 73–81, <https://doi.org/10.1016/J.ELECTACTA.2012.08.107>.
- [50] G. Beamon, D. Briggs, *High resolution XPS of organic polymers. The Scienta ESCA300 Database*, John Wiley & Sons, Ltd., Chichester, UK, 1992.
- [51] H. Kuzmany, A. Kukovecz, F. Simon, M. Holzweber, C. Kramberger, T. Pichler, Functionalization of carbon nanotubes, *Synth. Met.* 141 (2004) 113–122, <https://doi.org/10.1016/j.synthmet.2003.08.018>.
- [52] I.D. Rosca, F. Watari, M. Uo, T. Akasaka, Oxidation of multiwalled carbon nanotubes by nitric acid, *Carbon* 43 (2005) 3124–3131, <https://doi.org/10.1016/j.carbon.2005.06.019>.
- [53] A.G. Mahmoud, M.F.C. Guedes da Silva, A.J.L. Pombeiro, Organomanganese / amido-phosphine (DAPTA) catalyst for rapid cyanosilylation of aldehydes in glycerol and solvent-free conditions at room temperature, *Catal. Today* 418 (2023), 114056, <https://doi.org/10.1016/j.cattod.2023.114056>.
- [54] A. Bauzá, T.J. Mooibroek, A. Frontera, Tetrel bonding interactions, *Chem. Rec.* 16 (2016) 473–487, <https://doi.org/10.1002/TCR.201500256>.
- [55] A. Bauzá, S.K. Seth, A. Frontera, Tetrel bonding interactions at work: impact on tin and lead coordination compounds, *Coord. Chem. Rev.* 384 (2019) 107–125, <https://doi.org/10.1016/J.CCR.2019.01.003>.
- [56] A. Frontera, Tetrel bonding interactions involving carbon at work, *Recent Adv. Cryst. Eng. Catal.*, C. 6 (2020) 60, <https://doi.org/10.3390/C6040060>.
- [57] S. Scheiner, Origins and properties of the tetrel bond, *Phys. Chem. Chem. Phys.* 23 (2021) 5702–5717, <https://doi.org/10.1039/D1CP00242B>.
- [58] E. Atrián-Blasco, S. Gascón, M.J. Rodríguez-Yoldi, M. Laguna, E. Cerrada, Synthesis of Gold(I) derivatives bearing alkylated 1,3,5-triaza-7-phosphaadamantane as selective anticancer metalodrugs, *Eur. J. Inorg. Chem.* 2016 (2016) 2791–2803, <https://doi.org/10.1002/ejic.201600177>.
- [59] W.L.F. Armarego. *Purification of Laboratory Chemicals*, eighth ed., Elsevier, 2017 [https://doi.org/10.1016/s0022-328x\(00\)82974-5](https://doi.org/10.1016/s0022-328x(00)82974-5).
- [60] M.P. de Almeida, L.M.D.R.S. Martins, S.A.C. Carabineiro, T. Lauterbach, F. Rominger, A.S.K. Hashmi, A.J.L. Pombeiro, J.L. Figueiredo, Homogeneous and heterogenised new gold C-scorpionate complexes as catalysts for cyclohexane oxidation, *Catal. Sci. Technol.* 3 (2013) 3056–3069, <https://doi.org/10.1039/c3cy00552f>.